Creep Behaviour and Adhesion Properties of TiC Thin Film Coating Grown by RF Magnetron Sputtering

Abegunde Olayinka, Esther T. Akinlabi, and O. P. Oladijo

Abstract In this research study, the creep behaviour and adhesion resistance of TiC thin films grown using RF magnetron sputtering under different deposition parameters were investigated. Radio frequency (RF) magnetron sputter was used to coat the surface of CpTi with TiC target. Field electron scanning electron microscope was used to study the film morphology, and the hardness, young modulus, and creep behaviour tests were performed using TI 950 Triboindenter. The adhesion resistance property was investigated using a microscratch tester under ambient working condition. From the results, the TiC thin film morphology structures show different growth modes as the RF power changes. Films with uniform surface morphology show better adhesion resistance to peeling than films with high surface asperities, while films with heterogeneous distribution of the TiC thin films show high hardness values.

Keywords Acoustic emission · Creep · Mechanical properties · RF magnetron sputtering · Thin film

1 Introduction

Surface modification is an act of improving the surface performance of a material by coating the surface with different materials of better and improved quality. The performance functionality of this coating materials depends on the mechanical properties such as adhesion strength, hardness, young modulus, wear and creep resistance. There are several techniques used for surface modification, which depend on the materials' properties and area of applications. In recent years, there has been a

---

A. Olayinka (✉) · E. T. Akinlabi · O. P. Oladijo
University of Johannesburg, Johannesburg 2006, South Africa
e-mail: oabegunde@uj.ac.za

E. T. Akinlabi
Covenant University, Ota, Nigeria

O. P. Oladijo
Botswana International University of Science and Technology, Palapye, Botswana

paradigm shift in surface modification coating from age-old electroplating processes to new improved coating techniques such as chemical vapour deposition (CVD), physical vapour deposition (PVD), ion beam, vacuum arc deposition, evaporation, thermal spray, and pulsed laser ablation (PLD) [1–7]. One of the major considerations in using coating techniques is the adhesion bond between the substrate and the coating materials. Adequate bonding and adequate compatibility between the substrate and the film is an indication of good mechanical properties. Mechanical properties such as creep and adhesion strength are crucial to film failure under loading. Creep is the time-dependent deformation that occurs under application of load, and adhesion strength is the resistance of thin films peeling to applied normal or shear load. Strong adhesion bond yields good resistance to coating fracture under stationary or progressive loading and good creep resistance behaviour. The choice of the coating materials is also another influential factor that affects the final mechanical properties of the thin film coating. Titanium carbide TiC is one of the most widely applied hard coating materials due to its several advantageous and outstanding properties. These properties are high hardness, low coefficient of friction, outstanding wear resistance, high melting or decomposition temperature, good electrical conductivity, excellent corrosion resistance and chemical stability [8–13].

It is well known from studies that the properties of deposited titanium carbide thin films coatings depend strongly on the deposition conditions and coating techniques, and these properties are related to their chemical composition, texture, creep behaviour, residual stress and adhesion property [10]. However, the correlation between the creep resistance and adhesion behaviour and the process parameters (RF power and sputtering time) of RF magnetron sputtering still needs to be understood. In this research, RF magnetron sputtering was used to sputter TiC thin films by varying the RF power and sputtering time, and the relationship between the mechanical properties of the films and process parameters was studied.

2 Methodology

2.1 RF Magnetron Sputtering Process

TiC thin films were coated on commercially pure titanium (CpTi) using the process parameters presented in Table 1. HHV TF500 RF magnetron sputter was used for the

Table 1 RF magnetron process parameters

Experiment no	RF power (W)	Sputtering time (Hrs)
L1	150	2.5
L2	200	2.5
L3	200	3
L4	250	3

coating deposition. Before coating the substrate (CpTi) with TiC thin film, surface cleansing was done on the substrates to remove surface contaminants and uniform surface asperities. This was achieved by grounding and polishing using silica carbide papers of different grit sizes. The substrates were further cleaned using acetone, isopropanol and deionized water for 15 min, respectively. The distance between the substrate and target was maintained throughout the deposition process. Before the sputtering process commences, the sputtering chamber was first evacuated to a pressure of 1.13×10^{-5} mbar to provide a long mean free path for collision between the target and substrate and to minimize contaminants. After thorough evacuation of the chamber, the system was filled with argon to a partial pressure of 0.1–10 Pa to initiate the plasma formation and working temperature of 90 °C.

2.2 Characterization Techniques

Field emission scanning electron microscope FESEM (ZEISS Gemini*2, Germany) was used to analyse the film morphology. Images of the film morphology were taken at × 50,000 magnification. Hysitron TI 950 Triboindenter was used to evaluate the nanomechanical properties of the coating. The hardness and reduced young modulus were measured using a Berkovich diamond indenter, and they were calculated according to the method proposed by Oliver and Pharr [14, 15]. The Berkovich diamond indenter was preferred over the four-sided Vickers or Knoop indenter because a three-sided pyramid is more easily ground to a sharp point with high accuracy and minimal influence of the substrate properties on the coating. In order to avoid the combined coating plus substrate effect, penetration displacement was set to slightly less than 10% of the total coating thickness. In all indentation tests, a total of 10 indents were averaged to determine the mean hardness and reduced young modulus. The displacements were continuously recorded during the indentations. The penetration displacement of the indenter at maximum load (H_{MAX}) and the final displacement (HF), recorded in the unloading curve, were used to determine the percentage of elastic recovery (%R) and plasticity using Eq. 1 given below.

$$\%R = \frac{H_{\mathrm{MAX}} - \mathrm{HF}}{H_{\mathrm{MAX}}} \times 100 \tag{1}$$

Indentation creep testing was performed using the same Hysitron TI 950 Triboindenter. A constant load was applied to the indenter, and the change in indentation depth (size) was monitored as a function of time. Anton Paar (Micro Combo Tester, Austria) scratch tester was used to determine the films adhesion properties. The microscratch tester was coupled with an acoustic emission sensor which was used to determine when the film peels from the substrate. A Rockwell diamond ball with a radius of 100 μm was used for the microscratch test. For each measurement, the applied load was progressive from 50 mN to 2 N at a sliding speed of 2 mm/min and

sliding length of 1 mm. The displacement of the diamond ball was linear. All these experiments were carried out in an ambient atmospheric condition.

3   Result

3.1   Morphology Evolution

The film morphology under different process parameters obtained from the FESEM is presented in Fig. 1. From the structure, the geometry and distribution of the TiC thin films coating changes with both deposition power and time. Sparse and uneven distribution was noticed for sample produced at RF power of 150 W (sample L1). This shows an early stage in TiC film deposition on the substrate. As the power increased to 200 W (samples L2 and L3), the TiC thin film became dense and was uniformly distributed across the surface. Increase in RF power has been reported to result in faster ejection of atom from the target and high condensation of the atoms on the substrate surface. As the sputtering time increased for sample L3, the grain size of the film became finer. Formation of incomplete new TiC thin film layer was noticed as the power was increased further to 250 W. This phenomenal growth mode is similar to Stranski–Krastanov growth mechanism where both layer by layer and island growth of coating happen simultaneously.
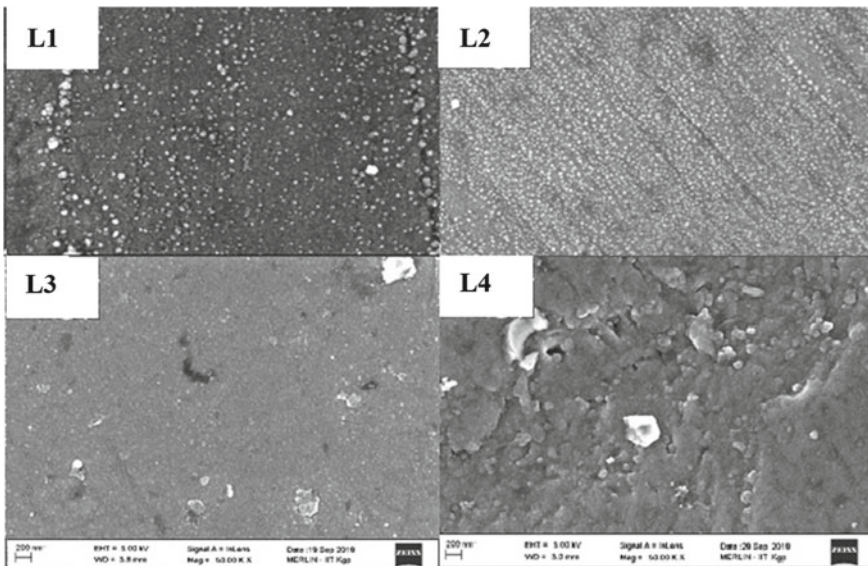

Fig. 1   FESEM morphology of TiC thin film coating

Table 2 Statistical results from the nanoindentation test

Sample	Young Modulus E (GPa)	Hardness H (GPa)	Wear resistance H^3/E^2 (GPa)	Plasticity index H/E	H_{MAX}	HF	%Recovery	Plasticity
L1	183.12	8.96	0.02	0.049	25.99	11.09	57.34	42.66
L2	115.55	4.77	0.0081	0.041	37.89	15.20	59.89	40.11
L3	119.11	5.75	0.013	0.048	35.07	13.03	62.83	37.17
L4	145.08	10.13	0.050	0.070	26.91	7.96	70.41	29.59

3.2 Mechanical Properties

Table 2 presents the results obtained from the nanohardness test, and Fig. 2 (a, b and c) shows the graphical representation of these results. The maximum hardness value was obtained at RF power of 250 W. This is due to increase in thickness and formation of several coating layers of TiC thin film when compared to other samples. The least hardness values were obtained at 200 W. The load vs displacement curve is presented in Fig. 2a. From the curve, samples with low hardness values yield
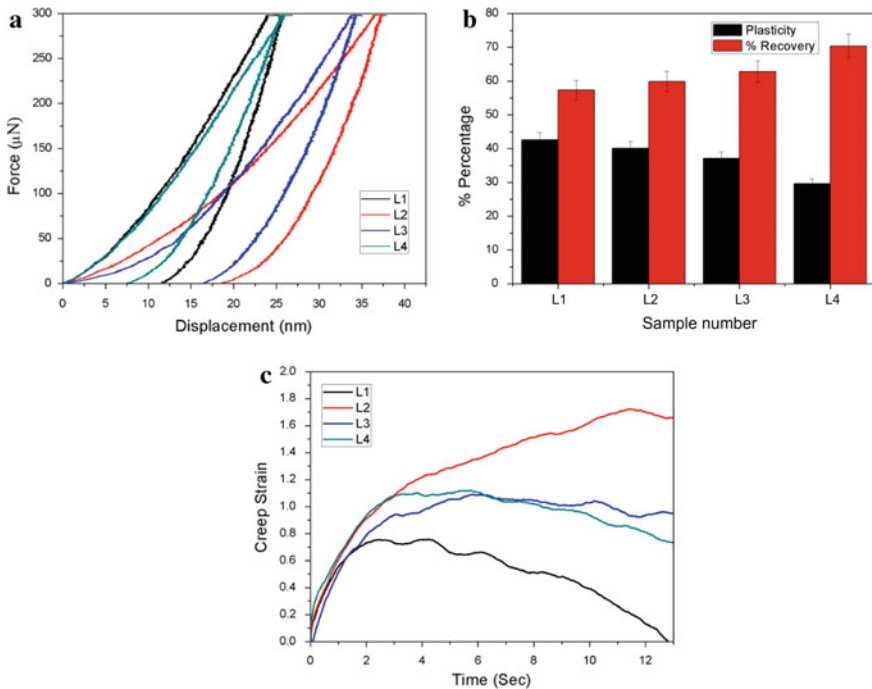

Fig. 2 a Force versus displacement curve. **b** Chart of the %recovery and plasticity. **c** Graph of creep strain versus time

the maximum displacement, and the displacement reduces as the hardness values increase. The %recovery and plasticity were calculated, and the graph is presented in Fig. 2b. From the results, the coating with the highest hardness value has the better %recovery and lowest plasticity. The %recovery increases with an increase in the RF power and sputtering time. This shows that the film plasticity and %recovery to deformation depend on the process parameters and thickness of the coating more than the hardness. To understand the creep behaviour, the plot of the creep strain against time is illustrated in Fig. 2c. From the plot, the depth displacement of the coating increases for 4 s for all the coated samples. Continued increase in creep strain was noticed for sample L2 with the lowest hardness while the other samples resisted the creep strain displacement and reduced with time. Samples with high creep were sign of thermal drift of the tip displacement and apparent depth increase, and samples with low creep were sign of resistance to deformation. As the hardness decreases, the creep strain increases. This shows that the hardness is inversely proportional to the creep behaviour.

The microscratch result is presented in Fig. 3. The plots show the applied force (Fn), acoustic emission (AE), coefficient of friction (COF), and penetration depth (Pd) against displacement. To understand the adhesion strength, the acoustic emission plot was used. Sudden spike in the plot of the acoustic emission means peeling of the thin film coating from the substrate and represents initialization of thin film failure. The films might either crack or resist the failure depending on the degree of the
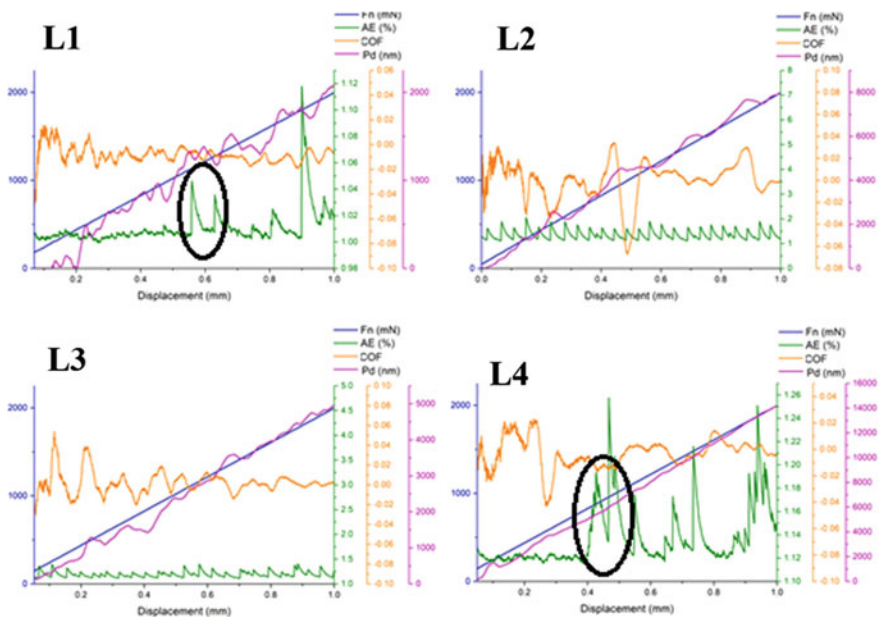

Fig. 3 Microscratch result of the TiC coatings. Plot of Applied force (Fn), Acoustic Emission (AE), Coefficient of friction (COF), penetration depth (Pd) against Displacement

applied load and the film properties. Samples L1 and L4 show signs of thin film failure from the acoustic emission plot. The minimum load, at which the films fail, is called the critical load L_c [16, 17]. The circled portion on the plots of L1 and L4 shown in Fig. 3 denotes the initial critical load that initiates fracture of coating on the substrate. The coating with the homogenous and uniform coating (L2 and L3) withstands the applied load.

4   Conclusions

From the analysis of the results, it can be concluded that the morphology and geometry of the films change with the RF power and sputtering time. The films with uniform and homogenous coating show better adhesion properties compared with samples with uneven distribution of the TiC thin film coating that experienced fracture under microscratch test. The maximum hardness was noticed at RF power of 250 W which had the maximum %recovery.

References

 1. Konyashin IY (1996) Thin TiCx films chemically vapour deposited onto cemented carbides from the TiCl4-CCl4-H2 mixture. Thin Solid Films 278(1–2):37–44
 2. Guzman L et al (1998) Process parameters optimization for TiN and TiC formation using reactive ion beam assisted deposition. Surf Coat Technol 100:500–502
 3. Voevodin A et al (1996) Combined magnetron sputtering and pulsed laser deposition of carbides and diamond-like carbon films. Appl Phys Lett 69(2):188–190
 4. Knotek O et al (1995) On Superstoichiometric Ti-C, Si-C and Ta-C PVD Coatings. MRS online proceedings library archive, vol 403
 5. D'alessio L et al (1998) Silicon supported TiC films produced by pulsed laser ablation," Appl Surf Sci 134(1–4):53–62
 6. Ding X et al (2001) Preferential orientation of titanium carbide films deposited by a filtered cathodic vacuum arc technique. Surf Coat Technol 138(2–3):301–306
 7. AbegundeOO et al (2019) Overview of thin film deposition techniques
 8. Pierson HO (1996) Handbook of refractory carbides and nitrides: properties, characteristics. Processing and Applications, William Andrew
 9. Vepřek S, Reiprich S (1995) A concept for the design of novel superhard coatings. Thin Solid Films 268(1–2):64–71
10. Mani A et al (2005) Effects of residual stress on the mechanical and structural properties of TiC thin films grown by RF sputtering. Surf Coat Technol 194(2–3):190–195
11. Mikmekovà E (2014) Enhanced properties of carbon based coatings
12. Wiklund U et al (2000) Evaluation of a flexible physical vapor deposited TiC–C coating system. Surf Coat Technol 124(2–3):154–161

13. Oláh N et al (2017) Mechanical characterization and corrosion behavior of protective TiC/amorphous C nanocomposite coating as surface thin film. Resolution and Discovery 2(1):13–22
14. Oliver WC, Pharr GM (2004) Measurement of hardness and elastic modulus by instrumented indentation: advances in understanding and refinements to methodology. J Mater Res 19(1):3–20
15. Oliver WC, Pharr GM (1992) An improved technique for determining hardness and elastic modulus using load and displacement sensing indentation experiments. J Mater Res 7(6):1564–1583
16. Covarel G et al (2012) Characterization of organic ultra-thin film adhesion on flexible substrate using scratch test technique. Surf Coat Technol 211:138–142
17. Boddaert X et al (2013) Organic ultrathin film adhesion on compliant substrate using scratch test technique. Thin Solid Films 528:194–198